eNeuro

Research Article: New Research | Disorders of the Nervous System

Intranasal Administration of Oxytocin Attenuates Social Recognition Deficits and Increases Prefrontal Cortex Inhibitory Post-Synaptic Currents following Traumatic Brain Injury

https://doi.org/10.1523/ENEURO.0061-21.2021

Cite as: eNeuro 2021; 10.1523/ENEURO.0061-21.2021

Received: 13 February 2021
Revised: 10 May 2021
Accepted: 14 May 2021

1. Intranasal Administration of Oxytocin Attenuates Social Recognition Deficits and Increases Prefrontal Cortex Inhibitory Post-Synaptic Currents following Traumatic Brain Injury

2. Oxytocin and Pediatric Traumatic Brain Injury

3. Avery Runyan[1], Dana Lengel[1], Jimmy W. Huh[3], Jessica R. Barson[1,2] and Ramesh Raghupathi[1,2]

[1]Program in Neuroscience, Graduate School of Biomedical Science and Professional Studies and [2]Department of Neurobiology and Anatomy, Drexel University College of Medicine, Philadelphia PA 19129 and [3]Department of Anesthesiology and Critical Care Medicine, Children's Hospital of Philadelphia, Philadelphia PA 19104

*AR and DL contributed equally to this manuscript.

4. Address correspondence to:

Ramesh Raghupathi, PhD
Department of Neurobiology and Anatomy
Drexel University College of Medicine
2900 Queen Lane, Philadelphia PA 19129
T: 215-991-8405
E-mail: rr79@drexel.edu

5. Article contains 38 pages.
6. Article contains 10 figures, 1 table, no multimedia files.
7. The abstract contains 220 words (limit 250)
8. The introduction contains 609 words (limit 650)
9. The discussion contains 1728 words (limit 1500 words)

10. Authors report no conflicts of interest.

11. These studies were supported, in part, by grants from the National Institutes of Health R01 NS110898 (JH and RR) and Commonwealth Universal Research Enhancement from the Pennsylvania Department of Health SAP 410-007-9710 (RR) and SAP 410-007-7079 (RR)

Abstract

Pediatric traumatic brain injury (TBI) results in heightened risk for social deficits that can emerge during adolescence and adulthood. A moderate TBI in male and female rats on postnatal day 11 (equivalent to children below the age of 3) resulted in impairments in social novelty recognition, defined as the preference for interacting with a novel rat compared to a familiar rat, but not sociability, defined as the preference for interacting with a rat compared to an object in the three-chamber test when tested at 4-weeks (adolescence) and 8-weeks (adulthood) post-injury. The deficits in social recognition were not accompanied by deficits in novel object recognition memory and were associated with a decrease in the frequency of spontaneous inhibitory postsynaptic currents (IPSC) recorded from pyramidal neurons within layer II/III of the medial prefrontal cortex (mPFC). Whereas TBI did not affect the expression of oxytocin (OXT) or the oxytocin Receptor (OXT-R) mRNAs in the hypothalamus and mPFC respectively, intranasal administration of OXT prior to behavioral testing was found to reverse impairments in social novelty recognition and increase IPSC frequency in the mPFC in brain-injured animals. These results suggest that TBI-induced deficits in social behavior may be linked to increased excitability of neurons in the mPFC and suggests that the regulation of GABAergic neurotransmission in this region as a potential mechanism underlying these deficits.

Significance Statement

Traumatic brain injury (TBI) occurs in approximately half a million children below the age of 14 each year, with children younger than 4 years old at heightened risk. A younger age at injury is associated with worse behavioral and psychosocial outcomes in pediatric TBI patients, particularly as children age into adolescence and adulthood. In this study, we explored the role of oxytocin in the long-term effects of pediatric TBI on social behaviors in adolescence and adulthood. The results indicate that intranasal administration of oxytocin (OXT) improves social outcomes following pediatric TBI, potentially by increasing inhibitory neurotransmission within the medial prefrontal cortex (mPFC) and provide novel support for the use of intranasal OXT treatment to mitigate social deficits in pediatric TBI patients.

Introduction

Nearly half a million children younger than 14 years old suffer from a traumatic brain injury (TBI) each year (Faul and Coronado, 2015). Pediatric TBI is associated with poor psychosocial outcomes in adolescence and young adulthood (Levin et al., 2004; Anderson et al., 2012; Rosema et al., 2012; Ryan et al., 2016), such as lower scores in communication, emotional perception, social skills, and fewer relationships (Ryan et al., 2014; Ryan et al., 2016; Douglas, 2020). Chronic social and behavioral difficulties are the most prevalent and disabling outcome of pediatric TBI patients (Zamani et al., 2020), although these psychosocial deficits have historically received less attention in preclinical pediatric TBI studies.

A few preclinical studies to date have investigated social behavior as an outcome after pediatric TBI. Closed head injury in juvenile (21-day-old) mice led to impaired social recognition using the three-chamber test at 4 weeks post-injury (adolescence) and deficits in sociability at 8 weeks following injury (adulthood) (Semple et al., 2012; Semple et al., 2017). Contusive brain trauma in neonate (14-day-old) rats resulted in both sociability and social recognition deficits 2 weeks following injury (Wei et al., 2016). The mechanisms underlying these social deficits following pediatric TBI are not fully understood. TBI in 21-day-old mice resulted in diminished neuronal arbor complexity within the medial prefrontal cortex (mPFC) at 8 weeks post-injury (Semple et al., 2017), a region that has been implicated in social processing in both rodents and humans (Ko, 2017). Oxytocin (OXT), a neuropeptide known to affect PFC function and social behavior (Gimpl and Fahrenholz, 2001), is involved in social bonding and trust (Tops et al., 2013). Administration of OXT is reported to improve social recognition deficits in mouse models of autism (Andari et al., 2010; Sala et al., 2011; Hara et al., 2017).

Transplantation of hypoxia-conditioned induced pluripotent stem cell-derived progenitor cells (iPSCs) shortly after neonate TBI in rats improved sociability and social recognition, which was associated with an increase in both OXT and OXT receptor (OXTR) levels in the injured cortex (Wei et al., 2016).

The majority of central nervous system OXT is produced within the paraventricular nucleus (PVN) in the hypothalamus (Knobloch et al., 2012), from which oxytocin producing neurons project to various brain regions including the mPFC (Bakos et al., 2018; Jurek and Neumann, 2018). Neuronally expressed OXTRs are G-protein coupled receptors which are typically coupled to $G_{\alpha q}$ and activate downstream signaling pathways involving protein kinase C (Bakos et al., 2018). Within the mPFC, OXTRs are predominantly expressed on inhibitory somatostatin neurons and have been implicated in the modulation of social behaviors (Nakajima et al., 2014). OXT has been found to increase spontaneous inhibitory postsynaptic currents (IPSCs) and the release of gamma aminobutyric acid (GABA) (Wrobel et al., 2010; Harden and Frazier, 2016). We previously demonstrated that TBI in 11-day-old rats results in an increase in spontaneous excitatory postsynaptic currents (EPSCs) and a concomitant decrease in spontaneous IPSCs in layer II/III pyramidal neurons within the mPFC (Lengel et al., 2020). Increasing excitatory currents in the PFC decreases social exploration in rodents (Yizhar et al., 2011; Bicks et al., 2015), suggesting that changes in excitation/inhibition balance within the medial PFC may be a mechanism underlying deficits in social behaviors following TBI.

The purpose of the current study was to define the extent of social behavior deficits following a moderate closed-head injury in the 11-day-old rat and to determine whether OXT treatment would reverse these deficits. To investigate whether the behavioral effects of OXT may be facilitated by its actions within the medial PFC, we measured the effects of bath

application of OXT on electrophysiological properties of medial PFC pyramidal neurons using whole cell patch clamp recordings.

Materials and Methods

Animals

All animal procedures were performed in accordance with the regulations of the Institutional Animal Care and Use Committee and followed the NIH Guide for the Care and Use of Laboratory Animals. Timed-pregnant (E20) female Sprague-Dawley rats were purchased from Charles River Laboratories, Inc. (Wilmington, MA) and gave birth in the animal facility (average litter size was between 11 and 13 pups). A caveat to the present study is that the stress of transportation may affect social behavior in the offspring. Animals were housed under a normal 12-hour light-dark cycle (lights on from 7:00 AM to 7:00 PM) with *ad libitum* access to standard rat chow and water. Age-matched male and female rats used as the familiar and novel rats in the three-chamber test were also purchased from Charles River and housed in the same room under the same conditions as the test subjects. The pups were weaned on postnatal day 21 and group housed under the same conditions. Animals were handled for 5-10 minutes at least 2-3 times per week prior to the start of behavioral assessment.

Traumatic Brain Injury

The model of moderate pediatric TBI used in this study was originally characterized by Raghupathi and Huh (2007) and was subsequently used in multiple studies (Hanlon et al., 2017, 2019; Lengel et al., 2020). Animals from each litter were randomly assigned to sham-injury or brain-injury groups. Sham (n=52) or brain injury (n=60) was administered on postnatal day 11, the neurological equivalent of a child below the age of 4 (Porterfield, 1994; Yager and Thornhill, 1997; Rice and Barone, 2000). Male and female rat pups were anesthetized using isoflurane (Patterson Veterinary, Greeley CO, 5% induction, 2-3% maintenance) and an incision was made to expose the skull. Animals were then placed in a plastic rodent restrainer (Braintree Scientific

Braintree MA) and moved onto the stage of an electronic controlled cortical impact device (eCCI, Custom Design, Richmond VA). The impactor tip was driven into the intact skull at a velocity of 5 m/s (3 mm distance from zero point, 100 ms dwell time) over the left lateral hemisphere midway between the bregma and lambda. After impact, the pup was placed in a supine position and the time until the pup righted itself onto all four paws was measured. After righting, pups were then placed back on isoflurane and examined for hematoma and skull fractures, and the incision was sutured closed. Sham-injured animals were surgically prepared but did not receive an impact. The total time under anesthesia for brain- and sham-injured animals did not exceed 10 minutes. Animals were placed in a separate cage to recover and were subsequently returned to the dam. Surgical procedures and recovery were performed on a heating pad to maintain the body temperature at 37ºC.

Behavioral Testing

All behavioral tests were conducted in the dark under red light with the three-chamber test being done first at 4 weeks or 8 weeks post-injury, followed by novel object recognition memory test (week 5 or week 9), and assessment of locomotor activity (week 6 for the oxytocin treatment arm of the study). All behaviors were recorded and testing and scoring from videos were performed by an evaluator who was blinded to the injury and treatment status of the animals.

Three-Chamber Test

Social behavior was quantified using a three-chamber test. Rats were tested 4 weeks or 8 weeks after injury. The three-chamber apparatus was custom made, comprised of three chambers with two Plexiglas dividers with a 10 cm opening to allow the rat to move between the 2 far chambers (40 x 40 cm) and a middle chamber (20 x 40 cm). A camera equipped with an infra-red detector was used to record the behavior of the test rat in each of the stages, from which the time

spent sniffing the rat/cup (stage 2), or the novel/familiar rat (stage 3), was determined. In the first stage, the rat was habituated to the three-chamber apparatus in the dark for five minutes following which it was herded into the middle chamber and the plexiglass doors were lowered to keep the animal in the middle chamber. In preparation for Stage 2, an age- and sex-matched rat that the test rat had never seen before was put in an inverted wire mesh cup (14 cm diameter, 20 cm height) in one of the outer chambers and an identical empty cup was placed in the opposite chamber. Stage 2, which measures sociability, began once the plexiglass doors were raised. This stage lasted ten minutes and the number of seconds the test rat spent sniffing the 'rat cup' and 'empty cup' was counted. At the end of this stage, the lights were turned on and the test rat was again herded back into the middle chamber and the plexiglass doors closed. Another new novel rat was placed in the empty cup. In Stage 3, social recognition was measured as the time the test rat spent sniffing the 'familiar rat' (from stage 2) and the 'novel rat' over ten minutes. The discrimination index (DI) in Stage 2 used the equation [(Time sniffing rat cup)-(Time sniffing empty cup)]/[(Time sniffing rat cup)+(Time sniffing empty cup)] and, for Stage 3, the equation [(Time sniffing novel rat)-(Time sniffing familiar rat)]/[(Time sniffing novel rat)+(Time sniffing familiar rat)].

Novel Object Recognition

To assess non-social memory, a novel object recognition paradigm was used. All testing and habituation occurred in the dark and the behaviors were recorded using a camera equipped with an infra-red detector. Rats were first habituated over two days to a plastic box (61 cm x 41 cm) for 10 minutes each day. On the third day, rats began the novel object recognition test by being familiarized with two identical objects placed in opposite corners of the box for 5 minutes. Rats were returned to their home cage, then returned one hour later to the box with one of the

objects switched for a new ("novel") object. The time the rat sniffed the 'familiar' object versus the 'novel' object was determined. Discrimination index (DI) was calculated using the following equation: [(Time sniffing novel object)-(Time sniffing familiar object)]/[(Time sniffing novel object)+(Time sniffing familiar object)].

Locomotor Activity

To assess any motor deficits, rats were tested individually in 43.2 cm x 43.2 cm activity monitor boxes (Activity Monitor Version 5, Med Associates, St. Albans, VT) during a 30-minute period. The total distance traveled, as tracked by the number of beam breaks, was measured and averaged in 5-minute bins for each animal.

Quantitative Real Time Polymerase Chain Reaction

At the conclusion of behavioral testing in adolescence (5 weeks post-injury), tissue from the PVN and PFC regions of a subset of rats (11 sham, 13 injured) were dissected after decapitation of male and female rats for quantitative real time polymerase chain reaction (qRT-PCR). For dissection of the PVN, coronal slices were obtained between -1.2 mm and -2.2 mm from bregma. For dissection of the PFC, coronal slices were obtained between +3.0 and +4.0 from bregma. The PVN was dissected as a reversed isosceles triangle, 1.0 mm bilateral to the third ventricle and between the fornix structures. The PFC was dissected in a diamond shape, bilateral from the dorsomedial tip of the slice to the corpus callosum, and then along the border of the corpus callosum to its ventral tip. Tissue was then stored in RNA Later (Qiagen Inc., Valenia, CA, USA) at -20°C until further processing. The RNA from the tissue was extracted using a RNeasy Mini Kit (Qiagen Inc.) along with DNase 1 (Qiagen Inc.). RNA yields were measured with a NanoDrop Lite spectrophotometer (Thermo Electron North America LLC,

Madison WI) and resulted in A_{260}/A_{280} ratios of 2.0 – 2.1, indicating high purity. RNA was converted to cDNA using SuperScript® VILO™ Master Mix (Invitrogen, Grand Island, NY, USA) in a SimpliAmp™ Thermal Cycler (Applied Biosystems, Waltham, MA, USA). Triplicate samples of cDNA, SYBR Green PCR reagent (Applied Biosystems, Grand Island, NY, USA), and target primer or cyclophilin primer were run on a 96-Well MicroAmp® Fast Optical Reaction Plates (Applied Biosystems). The protocol was set to be 2 min at 50 °C, 10 min at 95 °C, 40 cycles of 15 s at 95 °C, and 1 min at 60 °C. Primers were designed with the help of the NCBI Primer design tool (http://www.ncbi.nlm.nih.gov/tools/primer-blast/) and purchased from Invitrogen at ThermoFisher Scientific (Grand Island, NY, USA). Serial dilutions of primers were tested for specificity and efficiency on sham tissue of the respective regions. Only primers with one peak in the melt curve indicating good specificity were used. Efficiency was determined by serial dilutions of primers and graphing log of the dilutions against the threshold cycle (Ct) values. Target mRNA expression was quantified relative to cyclophilin-A using the relative quantification method ($\Delta\Delta C_T$), which was quantified using the following equation: $-2^{(\text{Average CT values of target gene-Average CT values of Cyclophilin-A})}$. We chose to use Cyclophilin-A as a reference gene in this study because it was reported to be a stable housekeeping gene in multiple brain injury paradigms (Langnaese et al., 2008; Swijsen et al., 2012; Timaru-Kast et al., 2015). The sequences for the primers were as follows: cyclophilin-A (cyc, 200 nM), Forward: 5'-GTGTTCTTCGACATCACGGCT-3', Reverse: 5'-CTGTCTTTGGAACTTTGTCTGCA-3'; Oxytocin (OXT, 200 nM), Forward: 5'-ATCTGCTGTAGCCCGGATGG-3', Reverse: 5'-GAAGGAAGCGCCCTAAAGGT-3'; Oxytocin Receptor (OXTR, 100 nM), Forward: 5'-GGGCCACCACAACGCAACGAG-3'; Reverse: 5'-AGACCGCCCAGCAATCGAAG-3'.

Intranasal Oxytocin Administration

The following intranasal administration protocol was adapted from (Brabazon et al., 2017) and (Meidahl et al., 2018). Six days prior to any behavioral intranasal OXT testing, rats began a protocol to familiarize them to receiving intranasal drops. On the first day, rats were placed into a DecapiCone® disposable rodent restrainer (Braintree Scientific, Braintree, MA) with the end sealed off but which allowed the rat to move relatively freely in the bag for 10 minutes. The next day, the rats were restrained in the nose cone and flipped on their back for 1 minute. From the third to fifth day ~3 drops of saline were intranasally given to each rat. To administer drops, rats were restrained in the DecapiCone® and flipped on their back. Drops of 6 µl of saline were pipetted using a micropipette into each naris. After the last drop, rats remained on their back for another minute to ensure the saline or OXT did not drip out. Animals that sneezed out all the drops were given additional drops to better acclimate them. On the day of testing, rats were given OXT (O4375, Sigma-Aldrich) or saline 1 hour before testing. Sham- and brain-injured rats were randomly assigned to receive either 20 µg or 60 µg of OXT (Hara et al., 2017; Meidahl et al., 2018), or saline.

Slice Preparation

All patch clamp recordings were done at the conclusion of behavioral testing in adolescence (Fig. 1). Rats were anesthetized with Euthasol (Patterson Veterinary, Richmond, VA) (100 mg/kg) and then transcardially perfused with 60 mL of oxygenated slicing artificial cerebrospinal fluid (aCSF) containing (in mM) sucrose 34, glucose 11, $NaHCO_3$ 24, KCl 2.5, NaH2PO4 1.25, $MgSO_4$ 10, and $CaCl_2$ 0.5 at pH 7.4. Brains were quickly removed and glued to the slicing stage of a vibrating microtome (Leica Microsystems), and 300 µM coronal slices containing the mPFC were cut between 3 and 4 mm anterior to bregma. Slices were incubated for

1 hour at 37ºC in oxygenated aCSF containing (in mM) NaCl 126, glucose 10, $NaHCO_3$ 26, KCl 2.5, NaH_2PO_4 1.25, $MgSO_4$ 1, and $CaCl_2$ 2 at pH 7.4. After incubation, the slices were allowed to equilibrate at room temperature for at least 1 hour prior to recording.

Whole-Cell Patch Clamp Electrophysiology

Brain slices were individually transferred to a recording chamber and continually perfused with oxygenated aCSF maintained at 34ºC. In a subset of recordings, OXT was added to the bath solution at a 1 μM concentration, as previously used (Harony-Nicolas et al., 2017). OXT was bathed onto a slice for 10 minutes prior to the beginning of recording and was maintained for the duration of recording (3-5 cells per slice). Using an Olympus BX51WI microscope and Samsung SCB-2001 camera, individual layer II/III pyramidal neurons were identified with infrared differential interference contrast imaging. Borosilicate glass patch pipettes were pulled to a resistance of 5-8 MΩ and filled with (in mM) K gluconate 128, HEPES 10, $CaCl_2$ 0.05, GTP 0.3, ATP 5, glucose 1, and NaCl 4 at pH 7.4 for whole-cell patch-clamp recordings of intrinsic excitability measures and for a subset of recordings of excitatory and inhibitory currents (n=18 sham cells and 23 injured cells). Additional whole-cell patch-clamp recordings of excitatory and inhibitory currents (n=14 sham cells and 21 injured cells) were obtained using an intracellular solution was used consisting of (in mM): Cs-Gluconate 110, CsCl 10, EGTA 1, $CaCl_2$ 1, HEPES 10, ATP-Mg 1, and adjusted to pH 7.3. Because there were no appreciable differences in the magnitude of injury-induced changes and the effects of OXT on either EPSCs or IPSCs, both sets of cellular physiology data were combined for statistical analyses. Whole-cell recordings were acquired using an axon MultiClamp 700A amplifier and PClamp 9.2 data acquisition software (Molecular Devices), digitized using a DigiData 1332A digitizer (Molecular Devices) at 10 kHz, and low-pass filtered at 1kHz. The access resistance was continuously monitored

during recordings, and the recording was stopped if it exceeded 25 MΩ. A. Only neurons with a membrane potential of at least -60 mV and an action potential (AP) overshoot greater than 0 mV were used in the analysis. If a neuron exhibited a non-accommodating, high-frequency spiking pattern in response to depolarizing current injections, it was deemed a fast-spiking interneuron and was excluded from further analysis. In voltage clamp mode, neurons were held at -70 mV to record spontaneous excitatory post synaptic currents (EPSCs) for 5 minutes, and then at 0 mV to record spontaneous inhibitory post synaptic currents (IPSCs), the reversal potentials for chloride ions and cations, respectively.

Measurement of Intrinsic Excitability and Synaptic Properties

The data were analyzed using ClampFit 10.5 (Molecular Devices, San Jose, CA). The resting membrane potential was measured as the average voltage immediately after whole-cell configuration was achieved. The input resistance, rheobase, action potential threshold, and action potential amplitude were measured from current clamp recordings, which consisted of a series of depolarizing current steps (duration = 1s) from -100 to 220 pA in 20 pA increments. Input resistance was determined from voltage responses to the first 4 hyperpolarizing steps (-100 to -80 pA). The rheobase current was determined as the minimal current needed to induce an action potential. The action potential threshold was measured as the voltage at the onset of an action potential. The action potential amplitude was measured as the difference between the threshold and the peak of an action potential. In voltage clamp traces the spontaneous EPSCs and spontaneous IPSCs were analyzed using an automated template-matching protocol. The mean spontaneous current frequency was calculated for each cell across the full duration of the recording.

292 *Statistical Analysis*

293 Statistical analyses were performed using Statistica version 7.0 (StatSoft, Tulsa OK). All
294 data sets were confirmed to contain a normal distribution and homogenous variances, as
295 indicated by a Shapiro-Wilk and Levene's test, respectively. An independent samples t-test was
296 used for comparisons between two means. For comparisons between more than two means, an
297 ANOVA was used. Post-hoc tests, when necessary were conducted using the Neuman-Keuls
298 correction. A p value < 0.05 was considered significant. Kolmogorov-Smirnov statistical analysis
299 was used to quantify differences among distributions (cumulative probability plots), in which
300 case a p value <0.005 was accepted as significant.
301

Results

Acute Response to Injury

All brain-injured animals exhibited a skull fracture and hematoma immediately following injury on postnatal day 11 (data not shown). Brain-injured animals exhibited an increase in the time to right themselves following the impact (Table 1; Injury; $F_{(1,108)}$=57, p=0.000 ANOVA), which did not differ between male and female rats (Sex; $F_{(1,108)}$=0.0005, p=0.98, ANOVA). Brain injury also caused a brief period of apnea which did not differ between male and female rats (Sex; $t_{(108)}$=0.14, p=0.88, Unpaired T-test). The latency of the righting reflex was similar in animals receiving saline, 20 µg oxytocin, and 60 µg oxytocin, confirming the randomization of animals to treatment groups (Table 1; Treatment; $F_{(2,39)}$=0.19, p=0.82, ANOVA).

Effects of pediatric TBI on Social Behaviors During Adolescence

Brain injury on postnatal day 11 did not result in impairments in sociability (stage 2) in adolescent brain-injured rats (**Fig. 2A, 2C**). Both sham- and brain-injured animals spent significantly more time interacting with the rat cup compared to an empty cup, as measured by total sniffing time (**Fig. 2A**); ($F_{(1,58)}$=191.8, p=0.00, ANOVA). The discrimination ratio during stage 2 was slightly but significantly higher in brain-injured rats compared to their sham-injured counterparts (**Fig. 2C**); ($F_{(1,29)}$=4.6, p=0.04, ANOVA) although the total time spent sniffing both stimuli during stage 2 did not differ between sham and injured rats (data not shown); ($F_{(1,29)}$=0.18, p=0.6, ANOVA). Brain-injured animals exhibited an impairment in social novelty recognition (stage 3) during adolescence (**Fig. 2B, 2D**). Statistical analysis of sniffing time during stage 3 revealed a significant interaction between injury status and stimulus (novel vs. familiar) (**Fig. 2B**); ($F_{(1,58)}$=6.3, p=0.01). Post-hoc tests showed that sham-injured animals spent significantly more time sniffing the novel rat compared to the familiar rat (p=0.005) and

compared to their brain-injured counterparts (p=0.02). In contrast, brain-injured rats did not exhibit a significant difference in the time sniffing a novel rat compared to a familiar rat (p=0.6). Statistical analysis also revealed that the discrimination index during stage 3 was significantly lower in brain-injured animals compared to sham-injured animals (**Fig. 2D**; $F_{(1,29)}$=4.75, p=0.03, ANOVA). The total time spent sniffing both stimuli during stage 3 did not differ between sham and injured rats (data not shown; $F_{(1,29)}$=2.4, p=0.12, ANOVA). Overall, these experiments demonstrate that brain-injured male and female rats exhibit impairments in social recognition but intact sociability at 4weeks post-injury.

Effects of pediatric TBI on Social Behaviors During Adulthood

Brain injury on postnatal day 11 did not result in impairments in sociability (stage 2) in adult brain-injured rats (**Fig. 3A, 3C**). Both sham- and brain-injured animals spent significantly more time interacting with the rat cup compared to an empty cup, as measured by total sniffing time (**Fig. 3A**; $F_{(1,32)}$=140.5, p=0.00). The discrimination ratio during stage 2 was not significantly different between sham- and brain-injured rats (**Fig. 3C**; $F_{(1,16)}$=0.1, p=0.7, ANOVA). The total time spent sniffing both stimuli during stage 2 also did not differ between sham and injured rats (data not shown, $F_{(1,16)}$=0.5, p=0.4, ANOVA). Brain-injured animals exhibited an impairment in social novelty recognition (stage 3) during adulthood (**Fig. 3B, 3D**). Statistical analysis revealed a significant interaction effect of injury status and the type of stimulus on total sniffing time (**Fig. 3B**; $F_{(1,32)}$=4.1, p=0.04). Post-hoc tests showed that sham-injured animals spent significantly more time sniffing the novel rat compared to the familiar rat (p=0.02), whereas brain-injured rats did not exhibit a significant difference in the time sniffing a novel rat compared to a familiar rat (p=0.5). Statistical analysis also revealed that the discrimination index during stage 3 was significantly lower in brain-injured animals compared to

sham-injured animals (**Fig. 3D**; $F_{(1,16)}$=4.6, p=0.04, ANOVA). The total time spent sniffing both stimuli during stage 3 was slightly but significantly higher in brain-injured rats compared to sham-injured rats (data not shown, $F_{(1,16)}$=5.6, p=0.03, ANOVA). Overall, these experiments demonstrate that brain-injured male and female rats exhibit impairments in social recognition but intact sociability at 8-weeks post-injury.

Novel Object Recognition During Adolescence and Adulthood

Brain injury did not result in an impairment in novel object recognition memory during either adolescence (**Fig. 4A**) or adulthood (**Fig. 4B**). Statistical analysis revealed no significant effect of injury status on the discrimination index at either 4-weeks ($F_{(1,29)}$=0.63, p=0.43, ANOVA) or 8-weeks post-injury ($F_{(1,9)}$=0.22, p=0.65, ANOVA). The sex of the animal did not have a significant effect on the discrimination index at either 4-weeks ($F_{(1,29)}$=0.19, p=0.66, ANOVA) or 8-weeks post-injury ($F_{(1,9)}$=0.06, p=0.81, ANOVA). Thus, these experiments confirm that TBI did not impair novel object recognition memory at either 4-weeks or 8-weeks post-injury.

Expression of mRNA for Oxytocin and Oxytocin Receptors

To determine whether TBI induces changes in the OXT system, we measured OXT and OXTR mRNA within the PVN and PFC, respectively (**Fig. 5A, 5B**). Statistical analysis revealed no significant effects of injury ($F_{(1,19)}$=0.25, p=0.62, ANOVA) or sex ($F_{(1,19)}$=0.04, p=0.83) on OXT mRNA within the PVN (**Fig. 5A**). Similarly, there was no significant effect of injury ($F_{(1,20)}$=2.11, p=0.16, ANOVA) or sex ($F_{(1,20)}$=0.22, p=0.64, ANOVA) on OXTR mRNA within the PFC (**Fig. 5B**). Thus, TBI did not induce changes in OXT expression within the PVN or in OXTR expression within the PFC.

Effects of Oxytocin Treatment on Social Behaviors and Novel Object Recognition Following TBI

To determine whether OXT treatment affects social behaviors after TBI, OXT (20 or 60 µg) was intranasally administered 30 minutes prior to testing in the three-chamber-test (**Fig. 6**). Oxytocin treatment did not have a significant effect on sniffing times during stage 2 (sociability) (**Fig. 6A**). Overall, rats spent more time sniffing the rat cup compared to the empty cup ($F_{(1,82)}$=360.8, p=0.00, ANOVA), regardless of injury status ($F_{(1,82)}$=0.3, p=0.5, ANOVA) or treatment ($F_{(2,82)}$=0.9, p=0.4, ANOVA). Interestingly, there was a significant effect of oxytocin treatment on the discrimination index during stage 2 (**Fig. 6C**; $F_{(2,41)}$=4.1, p=0.02). Post-hoc tests revealed that the discrimination index was significantly lower in animals treated with 60 µg OXT compared to both saline (p=0.02) and 20 µg OXT (p=0.04), although these animals still spent more time sniffing the rat cup compared to the empty cup (**Fig. 6A**), indicating intact sociability. Oxytocin treatment dose dependently increased social recognition (stage 3) in brain-injured animals (**Fig. 6B, 6D**). Statistical analysis of the discrimination index scores revealed a significant interaction between injury status and treatment (**Fig. 6D**; $F_{(2,38)}$=3.6, p=0.03). Post-hoc tests indicated that treatment with 60 µg OXT significantly increased the discrimination index in brain-injured rats compared with brain-injured rats receiving either saline (p=0.00) or 20 µg OXT (p=0.02). Oxytocin did not affect the total sniffing time during stage 3 (data not shown, $F_{(2,38)}$=2.2, p=0.1). Oxytocin treatment did not affect novel object recognition memory (data not shown). Overall, these experiments demonstrate that OXT dose-dependently increased social recognition in brain-injured animals without affecting non-social memory, with the higher 60 µg dose having the greatest effect on social recognition memory.

Effects of Oxytocin on Novelty-Induced Locomotor Activity

An ANOVA with repeated measured revealed that there was no significant effect of brain injury on the distance traveled during a 30-minute period (**Fig. 7**; $F_{(1,30)}$=0.09, p=0.75). Treatment with 60 µg oxytocin 30-mintutes prior to locomotor testing also did not affect the distance traveled during the 30-minute period ($F_{(1,30)}$=0.4, p=0.5, ANOVA). There was a main effect of time on the distance traveled ($F_{(5,150)}$=257.7, p=0.000, Repeated Measures ANOVA), with all animals exhibiting more activity during the first 5 minutes compared with the other time points (p<0.001), confirming the assessment of novelty-induced activity. Thus, these experiments confirm that neither TBI nor OXT treatment affected novelty-induced locomotor activity.

Whole Cell Patch Clamp Electrophysiology

Intrinsic Excitability of layer II/III neurons: Current clamp recordings from pyramidal cells from sham and brain-injured animals (illustrated in **Fig. 8A**) reveled a significant effect of TBI on input resistance (**Fig 8D**; $F_{(1,35)}$=4.6, p=0.03, ANOVA). The input resistance was significantly higher in neurons from brain-injured animals compared to their sham-injured counterparts (p=0.03) and was not affected by OXT ($F_{(1,35)}$=0.3, p=0.6, ANOVA). An increase in input resistance is typically associated with an increase in neuronal excitability. There was also a significant effect of TBI on the rheobase (**Fig 8A, 8C**; $F_{(1,36)}$=9.7, p=0.003, ANOVA), which was significantly decreased in neurons from brain-injured animals compared to sham animals (p=0.003), indicative of increased excitability, and was similarly not affected by OXT ($F_{(1,36)}$=0.01, p=0.9, ANOVA). However, there was no difference in the spike frequency in response to varying levels of current injection between the groups (**Fig 8B**, $F_{(2,27)}$=0.7, p=0.53, Repeated Measures ANOVA). There were no differences between cells recorded from sham and

brain-injured animals in the membrane voltage (**Fig 8E;** $F_{(1,35)}$=0.97, p=0.3, ANOVA), spike threshold (**Fig. 8F;** $F_{(1,37)}$=0.1.5, p=0.2, ANOVA), or spike amplitude ($F_{(1,37)}$=3.0, p=0.09, ANOVA, data not shown). Overall, these experiments indicate that TBI resulted in an increase in the excitability of layer II/III pyramidal cells which was not affected by OXT.

Excitatory Inputs to Layer II/III neurons: Representative traces of spontaneous excitatory postsynaptic currents (EPSCs) are illustrated in figure 9A. There were no significant differences in either the frequency (**Fig. 9B;** $F_{(1,58)}$=3.1, p=0.08, ANOVA) or amplitude (**Fig. 9C;** $F_{(1,60)}$=2.3 p=0.1, ANOVA) of spontaneous EPSCs between sham-injured cells and brain-injured cells recorded with either aCSF or OXT. Thus, there were no significant effects of either TBI or OXT application on excitatory inputs to layer II/III neurons.

Inhibitory Inputs to Layer II/III neurons: Representative traces of spontaneous inhibitory postsynaptic currents (IPSCs) are illustrated in figure 10A. There was a significant interaction effect on the frequency of spontaneous IPSCs (StatusXTreatment; $F_{(1,49)}$=5.6, p=0.02, ANOVA). Post-hoc tests revealed that IPSC frequency was significantly lower in cells from brain-injured animals recorded with ACSF relative to cells from sham-injured animals (p=0.008) and cells from brain-injured animals recorded in the presence of OXT (p=0.02) (**Fig. 10B**). There was no difference in the IPSC frequency in sham cells bathed with either aCSF or OXT (p=0.49). However, there were no effects of TBI ($F_{(1,49)}$=1.3, p=0.25, ANOVA) or OXT ($F_{(1,49)}$=0.0006, p=0.98, ANOVA) on the amplitude of spontaneous IPSCs (**Fig 10C**). There were no effects of sex on the frequency ($F_{(1,49)}$=0.64, p=0.4, ANOVA) or amplitude ($F_{(1,49)}$=2.7, p=0.1, ANOVA) of IPSCs recorded from layer II/III.

Because IPSCs evoked by somatostatin-expressing interneurons, which typically project to distal dendrites of pyramidal neurons (Urban-Ciecko and Barth, 2016), are smaller compared to

parvalbumin-expressing interneurons (Holley et al., 2019), cumulative probability analyses on the amplitudes and frequencies of either small (<20 pA) or large (<60 pA) IPSCs were performed. A Kolmogorov-Smirnov test revealed a significant difference in the distribution of frequencies of both small IPSCs ($D_{(43)}$=0.67, p<0.001) and large IPSCs ($D_{(572)}$=0.33, p<0.001) between sham and injured mPFC cells bathed with aCSF (**Fig. 10D-10G**). Bath application of OXT led to a rightward shift in the distribution of frequencies of both small IPSCs ($D_{(140)}$=0.37, p<0.005) and large IPSCs ($D_{(428)}$=0.27, p<0.001) in brain-injured cells (**Fig. 10E, 10G**) but did not affect either small IPSCs ($D_{(204)}$=0.33, p>0.1) or large IPSCs ($D_{(744)}$=0.06, p>0.1) in sham cells (**Fig. 10D, 10F**). There was no effect of TBI on the amplitude of either small IPSCs ($D_{(75)}$=0.27, p>0.1) or large IPSCs ($D_{(349)}$=0.08, p>0.1) in cells bathed with aCSF, although bath application of OXT led to a leftward shift in the distribution of amplitudes of small IPSCs in brain-injured cells ($D_{(205)}$=0.36, p<0.001, **Fig. 10I**), without affecting large IPSC amplitudes ($D_{(436)}$=0.13, p>0.1, **Fig. 10K**). Moreover, OXT did not affect the amplitudes of either small IPSCs ($D_{(236)}$=0.22, p>0.1) or large IPSCs ($D_{(1150)}$=0.05, p>0.1) in sham cells **(Fig. 10H, 10J).**

Overall, these experiments indicate that TBI resulted in a significant decrease in the frequency of IPSCs recorded from layer II/III pyramidal neurons, and that bath-application of OXT increased the IPSC frequency in pyramidal cells from brain-injured animals without having an overall effect on IPSC amplitude. Moreover, OXT increased the frequency of IPSCs of both small and large amplitudes but had a selective effect on the amplitudes of small IPSCs in mPFC neurons from brain-injured animals.

Discussion

The present study demonstrates that moderate TBI in the 11-day-old rat resulted in social recognition deficits at 4- and 8-weeks post-injury, corresponding to adolescence and adulthood, respectively. Intranasal administration of oxytocin (OXT) prior to behavioral testing reversed social recognition deficits in brain-injured animals. Closed-head injury did not affect sociability in the three-chamber test or novel object recognition memory, indicating that these deficits were specific to the neural circuits underlying social memory rather than recognition memory in general. Moreover, brain-injured animals exhibited a significant increase in excitability and decrease in the frequency of spontaneous IPSCs in layer II/III PFC pyramidal neurons, which was consistent with previous results (Lengel et al., 2020) Bath application of OXT increased IPSC frequency but did not affect neuronal excitability. Overall, these findings suggest that oxytocin improves social recognition memory following pediatric TBI, and that this effect may be mediated by the facilitation of inhibitory neurotransmission within the PFC by OXT.

The findings from this study differ from previous studies demonstrating changes in social behaviors following pediatric TBI. Semple et. al. found that contusive brain trauma in 21-day-old mice resulted in deficits in sociability and preference for social novelty during adulthood (p60-p70), but not adolescence (p35-p42) (Semple et al., 2012). Another study reported deficits in both sociability and social novelty preference during adolescence (p31) following controlled cortical impact (CCI) in 14-day-old rats (Wei et al., 2016). These seemingly inconsistent results are likely due to a variety of factors including age at time of injury, injury model, and species. While we did not observe sex differences in the effects of TBI on social behaviors, Semple et. al. found that while male mice injured on postnatal day 21 exhibited deficits in both sociability and preference for social novelty in adulthood, female mice exhibited reduced sociability but intact

preference for social novelty (Semple et al., 2017). Moreover, these sex-dependent changes were associated with a reduction in dendritic complexity within the PFC and hippocampus that was more apparent in males and preceded the onset of social impairments (Semple et al., 2017). Although evidence of neuronal death or neurodegeneration within the mPFC, has not been observed (Lengel et al., 2020), changes in dendritic morphology following TBI may be a potential mechanism underlying changes in the excitatory/inhibitory balance within the mPFC.

Our results demonstrate that oxytocin improves social recognition following TBI, which corroborate previous evidence that improvements in social behaviors mediated by iPSC transplantation following CCI are associated with higher levels of OXT and OXTR (Wei et al., 2016). The lack of an effect of OXT on social behaviors in sham animals in the current study supports previous findings in which OXT did not affect social novelty in wild-type mice and only increased preference for social novelty in mice that exhibit autism-like behaviors (Zhang et al., 2016; Hara et al., 2017). The ability of OXT to improve social recognition in brain-injured animals may be related to its ability to regulate GABAergic activity. TBI resulted in a reduction in the frequency but not amplitude of spontaneous IPSCs in the mPFC, which could implicate pre-synaptic changes in inhibitory neurotransmission. An imbalance of the cortical excitation/inhibition balance has been previously implicated in adult TBI (Witgen et al., 2005; Bonislawski et al., 2007; Ding et al., 2011; Cantu et al., 2015; Carron et al., 2016; Brizuela et al., 2017; Witkowski et al., 2019) and has been linked to reductions in inhibitory neurotransmission (Witgen et al., 2005; Bonislawski et al., 2007; Cantu et al., 2015; Carron et al., 2016). OXTRs within the PFC are expressed on regular-spiking somatostatin neurons (Nakajima et al., 2014), which synapse with pyramidal neurons in layer II/III (Urban-Ciecko and Barth, 2016). Although reductions in the numbers of somatostatin-containing inhibitory interneurons have been reported

503 following moderate TBI in adult rats (Carron et al., 2020), a previous study reported that
504 pediatric TBI does not result in neuron loss in the mPFC (Lengel et al., 2020).

505 Bath application of OXT in the present study was found to increase the IPSC frequency
506 but not amplitude in brain-injured PFC slices, suggesting that the effect of OXT on IPSCs were
507 likely mediated through the regulation of GABA release from inhibitory interneurons synapsing
508 with pyramidal neurons, rather than acting directly upon OXTRs on pyramidal neurons. These
509 effects of OXT were specifically observed in pyramidal neurons from brain-injured but not sham
510 slices. Although the effects of OXT on IPSC frequency in prefrontal cortex pyramidal neurons
511 have not previously been investigated, a previous study reported an increase in IPSC frequency
512 recorded from mossy cells in the dentate gyrus with application of the OXTR agonist, TGOT
513 (Harden and Frazier, 2016). In part, this differential response to TGOT may reflect its higher
514 specificity for the OXTR over the vasopressin receptor compared to OXT (Harden and Frazier,
515 2016). This observation also suggests that OXTRs in the mPFC may be exhibit higher sensitivity
516 for OXT following TBI, possibly due to a decrease in basal OXT levels, resulting in greater
517 OXTR activation by exogenous OXT in injured cells relative to sham cells.

518 Because OXTRs are predominantly expressed on somatostatin neurons in the mPFC
519 (Nakajima et al., 2014), which evoke smaller IPSCs in pyramidal neurons compared to
520 parvalbumin neurons (Holley et al., 2019), we predicted that OXT would preferentially affect the
521 frequency and/or amplitude of small IPSCs. While OXT significantly increased the frequency of
522 both small and large IPSCs in injured cells, it selectively affected the amplitudes of small IPSCs
523 resulting in a leftward shift in the distribution of small IPSC amplitudes recorded from injured
524 cells, suggestive of an increase in the number of smaller currents relative to larger currents. The
525 beneficial effects of OXT on social recognition may therefore be a result of increasing

GABAergic release from terminals of GABAergic neurons, including somatostatin and likely parvalbumin interneurons as well. Thus, although beyond the scope of this study, measuring the direct effects of OXT bath application on the activity of somatostatin and parvalbumin interneurons following TBI will be an important area of future investigation.

In contrast to a previous study (Lengel et al., 2020), we did not observe changes in spontaneous EPSC frequency in layer II/III pyramidal neurons in the mPFC. This may be due to differences in the timing of electrophysiological recordings, which were conducted at the conclusion of behavioral testing (between 6-7 weeks post-injury) in the current study. However, we did observe an increase in neuronal excitability (increase in input resistance and decrease in rheobase) and a reduction in spontaneous IPSC frequency, corroborating our previous findings and suggesting the effects of TBI on layer II/III EPSCs may be transient. In contrast, our current data indicate that the effects of TBI on layer II/III IPSCs are sustained up to 7 weeks following injury. We previously identified changes in the excitatory amino acid transporter 3 (EAAT3) and voltage-gated sodium channel β3-subunit (NaVβ3) as potential mechanisms underlying the effects on cellular function by progesterone treatment during the first week following injury (Lengel et al., 2020). In the present study, because the OXT was administered 30 minutes prior to behavioral testing, it is more likely that its effects were mediated through acute changes in signal transduction, rather than transcriptional changes or anti-inflammatory effects of oxytocin. Furthermore, whereas progesterone was found to predominantly affect neuronal excitability and excitatory neurotransmission, the findings from this study suggest that the behavioral effects of OXT may be specifically mediated through its effects on inhibitory neurotransmission (Harden and Frazier, 2016).

548 We did not observe changes in OXT mRNA in the hypothalamic paraventricular nucleus
549 (PVN) or OXTR mRNA in the PFC. Although expression of OXT and OXTR proteins were not
550 measured in the current study, a previous study reported no changes in OXT or OXTR protein
551 concentrations at 2 weeks following TBI in 14-day-old rats (Wei et al., 2016). Nonetheless, TBI
552 may influence important developmental processes that occur during the first postnatal weeks.
553 Notably, the maturation of OXT-producing neurons in the rat hypothalamus occurs later
554 compared with other neuropeptides including vasopressin (AVP) and somatostatin (SOM), with
555 OXT mRNA levels reaching about half of the adult levels during the third postnatal week
556 (Almazan et al., 1989). Moreover, this upregulation in gene expression occurs concomitantly
557 with the establishment of synaptic input to the PVN and the development of output projections
558 from the PVN to target regions during the first 2 postnatal weeks (Almazan et al., 1989). Thus, it
559 is possible that TBI leads to a loss of PVN projections to the mPFC, resulting in a reduction in
560 OXT release in the mPFC and, in turn, a decrease in the basal activation of OXTRs on these
561 neurons. A loss of basal OXT transmission in the mPFC could also explain the selective effect of
562 OXT administration in injured but not in sham cells, where there may be higher levels of
563 endogenous OXT release.

564 Although changes in OXT or OXTR mRNA were not observed at 6 weeks after injury,
565 we cannot rule out the possibility of transient changes in TBI-induced expression of these genes
566 at earlier time-points following injury. The hallmark of pediatric TBI is diffuse (traumatic)
567 axonal injury (Kannan et al., 2014) which has been validated in our model (Raghupathi and Huh,
568 2007). Moreover, although histopathological damage within the mPFC following pediatric TBI
569 has not been observed (Lengel et al., 2020), it is possible that the PVN OXT neurons that project
570 to the mPFC may be injured, resulting in impaired transmission of OXT to the mPFC and/or

other areas involved in social recognition. It is also important to acknowledge the existence of cross-reactivity between OXT and other neuropeptide systems such as vasopressin (Song and Albers, 2018), and thus the possibility that the beneficial effects of OXT treatment may have been partly mediated by vasopressin receptors. Thus, the molecular mechanism underlying the effects of OXT treatment on social recognition deficits following closed head injury remain a topic for further exploration.

In the present study we did not observe an impairment in novel object recognition memory following a single closed-head injury in the 11-day-old rat, which differs from previously published data in the neonate rat (Lengel et al., 2020). This discrepancy is likely due to differences in the testing conditions; in the present study animals were tested for novel object recognition under dark conditions, in contrast to the previous study in which they were tested under normal light conditions. Dark lighting conditions were used for novel object recognition testing in the present study in order to maintain the consistency of testing conditions between the novel object recognition test and three-chamber-test. We chose to test animals in the three-chamber test in dark conditions to avoid anxiogenic effects of excessive room lighting, which can influence the activity of animals behaving in the three-chamber test (Kaidanovich-Beilin et al., 2011).

A limitation of this study is that we did not measure changes in olfaction following TBI. Thus, we cannot rule out the possibility that the observed deficits in social novelty recognition may have been influenced by impairments in olfactory discrimination in brain-injured animals. However, the absence of deficits in sociability (stage 2) would suggest that olfaction may not be adversely affected by TBI. Moreover, a similar study reported sensory deprivation-induced social memory deficits despite normal olfaction, sociability, locomotor activity, and novel object

recognition memory (Zhang et al., 2016), confirming that impairments in social behaviors can occur independent of impairments in olfaction.

Overall, these findings demonstrate that a closed head injury in 11-day-old rats results in social recognition deficits which are accompanied by alterations in neuronal functionality within the mPFC. Further, we have identified the regulation of GABAergic neurotransmission within the PFC as a potential mechanism of these effects of OXT on social behaviors. Intranasal OXT treatment has shown promise in improving social deficits in children with autism (Parker et al., 2017). To the best of our knowledge, this is the first study to demonstrate beneficial effects of OXT administration on social behavioral outcomes following TBI in pediatric animals. Our findings provide support for the potential of intranasal OXT treatment as an effective therapeutic strategy for social deficits following pediatric TBI.

References

Almazan G, Lefebvre DL, Zingg HH (1989) Ontogeny of hypothalamic vasopressin, oxytocin and somatostatin gene expression. Brain Res Dev Brain Res 45:69-75.

Andari E, Duhamel JR, Zalla T, Herbrecht E, Leboyer M, Sirigu A (2010) Promoting social behavior with oxytocin in high-functioning autism spectrum disorders. Proc Natl Acad Sci U S A 107:4389-4394.

Anderson V, Godfrey C, Rosenfeld JV, Catroppa C (2012) 10 years outcome from childhood traumatic brain injury. Int J Dev Neurosci 30:217-224.

Bakos J, Srancikova A, Havranek T, Bacova Z (2018) Molecular Mechanisms of Oxytocin Signaling at the Synaptic Connection. Neural Plast 2018:4864107.

Bicks LK, Koike H, Akbarian S, Morishita H (2015) Prefrontal Cortex and Social Cognition in Mouse and Man. Front Psychol 6:1805.

Bonislawski DP, Schwarzbach EP, Cohen AS (2007) Brain injury impairs dentate gyrus inhibitory efficacy. Neurobiol Dis 25:163-169.

Brabazon F, Wilson CM, Jaiswal S, Reed J, Frey WHN, Byrnes KR (2017) Intranasal insulin treatment of an experimental model of moderate traumatic brain injury. J Cereb Blood Flow Metab 37:3203-3218.

Brizuela M, Blizzard CA, Chuckowree JA, Pitman KA, Young KM, Dickson T (2017) Mild Traumatic Brain Injury Leads to Decreased Inhibition and a Differential Response of Calretinin Positive Interneurons in the Injured Cortex. J Neurotrauma 34:2504-2517.

Cantu D, Walker K, Andresen L, Taylor-Weiner A, Hampton D, Tesco G, Dulla CG (2015) Traumatic Brain Injury Increases Cortical Glutamate Network Activity by Compromising GABAergic Control. Cereb Cortex 25:2306-2320.

Carron SF, Alwis DS, Rajan R (2016) Traumatic Brain Injury and Neuronal Functionality Changes in Sensory Cortex. Front Syst Neurosci 10:47.

Carron SF, Sun M, Shultz SR, Rajan R (2020) Inhibitory neuronal changes following a mixed diffuse-focal model of traumatic brain injury. J Comp Neurol 528:175-198.

Ding MC, Wang Q, Lo EH, Stanley GB (2011) Cortical excitation and inhibition following focal traumatic brain injury. J Neurosci 31:14085-14094.

Douglas J (2020) Loss of friendship following traumatic brain injury: A model grounded in the experience of adults with severe injury. Neuropsychol Rehabil 30:1277-1302.

Faul M, Coronado V (2015) Epidemiology of traumatic brain injury. Handb Clin Neurol 127:3-13.

Gimpl G, Fahrenholz F (2001) The oxytocin receptor system: structure, function, and regulation. Physiol Rev 81:629-683.

Hanlon LA, Raghupathi R, Huh JW (2017) Differential effects of minocycline on microglial activation and neurodegeneration following closed head injury in the neonate rat. Exp Neurol 290:1-14.

Hanlon LA, Raghupathi R, Huh JW (2019) Depletion of microglia immediately following traumatic brain injury in the pediatric rat: Implications for cellular and behavioral pathology. Exp Neurol 316:39-51.

Hara Y, Ago Y, Higuchi M, Hasebe S, Nakazawa T, Hashimoto H, Matsuda T, Takuma K (2017) Oxytocin attenuates deficits in social interaction but not recognition memory in a prenatal valproic acid-induced mouse model of autism. Horm Behav 96:130-136.

Harden SW, Frazier CJ (2016) Oxytocin depolarizes fast-spiking hilar interneurons and induces GABA release onto mossy cells of the rat dentate gyrus. Hippocampus 26:1124-1139.

650 Harony-Nicolas H, Kay M, du Hoffmann J, Klein ME, Bozdagi-Gunal O, Riad M, Daskalakis NP,
651 Sonar S, Castillo PE, Hof PR, Shapiro ML, Baxter MG, Wagner S, Buxbaum JD (2017)
652 Oxytocin improves behavioral and electrophysiological deficits in a novel Shank3-
653 deficient rat. Elife 6.
654 Holley SM, Galvan L, Kamdjou T, Dong A, Levine MS, Cepeda C (2019) Major Contribution of
655 Somatostatin-Expressing Interneurons and Cannabinoid Receptors to Increased GABA
656 Synaptic Activity in the Striatum of Huntington's Disease Mice. Front Synaptic Neurosci
657 11:14.
658 Jurek B, Neumann ID (2018) The Oxytocin Receptor: From Intracellular Signaling to Behavior.
659 Physiol Rev 98:1805-1908.
660 Kaidanovich-Beilin O, Lipina T, Vukobradovic I, Roder J, Woodgett JR (2011) Assessment of
661 social interaction behaviors. J Vis Exp.
662 Kannan N, Ramaiah R, Vavilala MS (2014) Pediatric neurotrauma. Int J Crit Illn Inj Sci 4:131-
663 137.
664 Knobloch HS, Charlet A, Hoffmann LC, Eliava M, Khrulev S, Cetin AH, Osten P, Schwarz MK,
665 Seeburg PH, Stoop R, Grinevich V (2012) Evoked axonal oxytocin release in the central
666 amygdala attenuates fear response. Neuron 73:553-566.
667 Ko J (2017) Neuroanatomical Substrates of Rodent Social Behavior: The Medial Prefrontal Cortex
668 and Its Projection Patterns. Front Neural Circuits 11:41.
669 Langnaese K, John R, Schweizer H, Ebmeyer U, Keilhoff G (2008) Selection of reference genes
670 for quantitative real-time PCR in a rat asphyxial cardiac arrest model. BMC Mol Biol 9:53.
671 Lengel D, Huh JW, Barson JR, Raghupathi R (2020) Progesterone treatment following traumatic
672 brain injury in the 11-day-old rat attenuates cognitive deficits and neuronal
673 hyperexcitability in adolescence. Exp Neurol 330:113329.
674 Levin HS, Zhang L, Dennis M, Ewing-Cobbs L, Schachar R, Max J, Landis JA, Roberson G,
675 Scheibel RS, Miller DL, Hunter JV (2004) Psychosocial outcome of TBI in children with
676 unilateral frontal lesions. J Int Neuropsychol Soc 10:305-316.
677 Meidahl AC, Eisenried A, Klukinov M, Cao L, Tzabazis AZ, Yeomans DC (2018) Intranasal
678 Oxytocin Attenuates Reactive and Ongoing, Chronic Pain in a Model of Mild Traumatic
679 Brain Injury. Headache 58:545-558.
680 Nakajima M, Gorlich A, Heintz N (2014) Oxytocin modulates female sociosexual behavior
681 through a specific class of prefrontal cortical interneurons. Cell 159:295-305.
682 Parker KJ, Oztan O, Libove RA, Sumiyoshi RD, Jackson LP, Karhson DS, Summers JE, Hinman
683 KE, Motonaga KS, Phillips JM, Carson DS, Garner JP, Hardan AY (2017) Intranasal
684 oxytocin treatment for social deficits and biomarkers of response in children with autism.
685 Proc Natl Acad Sci U S A 114:8119-8124.
686 Porterfield SP (1994) Vulnerability of the developing brain to thyroid abnormalities:
687 environmental insults to the thyroid system. Environ Health Perspect 102 Suppl 2:125-130.
688 Raghupathi R, Huh JW (2007) Diffuse brain injury in the immature rat: evidence for an age-at-
689 injury effect on cognitive function and histopathologic damage. J Neurotrauma 24:1596-
690 1608.
691 Rice D, Barone S, Jr. (2000) Critical periods of vulnerability for the developing nervous system:
692 evidence from humans and animal models. Environ Health Perspect 108 Suppl 3:511-533.
693 Rosema S, Crowe L, Anderson V (2012) Social function in children and adolescents after
694 traumatic brain injury: a systematic review 1989-2011. J Neurotrauma 29:1277-1291.

695 Ryan NP, Catroppa C, Godfrey C, Noble-Haeusslein LJ, Shultz SR, O'Brien TJ, Anderson V,
696 Semple BD (2016) Social dysfunction after pediatric traumatic brain injury: A translational
697 perspective. Neurosci Biobehav Rev 64:196-214.
698 Ryan NP, Anderson V, Godfrey C, Beauchamp MH, Coleman L, Eren S, Rosema S, Taylor K,
699 Catroppa C (2014) Predictors of very-long-term sociocognitive function after pediatric
700 traumatic brain injury: evidence for the vulnerability of the immature "social brain". J
701 Neurotrauma 31:649-657.
702 Sala M, Braida D, Lentini D, Busnelli M, Bulgheroni E, Capurro V, Finardi A, Donzelli A, Pattini
703 L, Rubino T, Parolaro D, Nishimori K, Parenti M, Chini B (2011) Pharmacologic rescue of
704 impaired cognitive flexibility, social deficits, increased aggression, and seizure
705 susceptibility in oxytocin receptor null mice: a neurobehavioral model of autism. Biol
706 Psychiatry 69:875-882.
707 Semple BD, Canchola SA, Noble-Haeusslein LJ (2012) Deficits in social behavior emerge during
708 development after pediatric traumatic brain injury in mice. J Neurotrauma 29:2672-2683.
709 Semple BD, Dixit S, Shultz SR, Boon WC, O'Brien TJ (2017) Sex-dependent changes in neuronal
710 morphology and psychosocial behaviors after pediatric brain injury. Behav Brain Res
711 319:48-62.
712 Song Z, Albers HE (2018) Cross-talk among oxytocin and arginine-vasopressin receptors:
713 Relevance for basic and clinical studies of the brain and periphery. Front Neuroendocrinol
714 51:14-24.
715 Swijsen A, Nelissen K, Janssen D, Rigo JM, Hoogland G (2012) Validation of reference genes for
716 quantitative real-time PCR studies in the dentate gyrus after experimental febrile seizures.
717 BMC Res Notes 5:685.
718 Timaru-Kast R, Herbig EL, Luh C, Engelhard K, Thal SC (2015) Influence of Age on Cerebral
719 Housekeeping Gene Expression for Normalization of Quantitative Polymerase Chain
720 Reaction after Acute Brain Injury in Mice. J Neurotrauma 32:1777-1788.
721 Tops M, Huffmeijer R, Linting M, Grewen KM, Light KC, Koole SL, Bakermans-Kranenburg
722 MJ, van Ijzendoorn MH (2013) The role of oxytocin in familiarization-habituation
723 responses to social novelty. Front Psychol 4:761.
724 Urban-Ciecko J, Barth AL (2016) Somatostatin-expressing neurons in cortical networks. Nat Rev
725 Neurosci 17:401-409.
726 Wei ZZ, Lee JH, Zhang Y, Zhu YB, Deveau TC, Gu X, Winter MM, Li J, Wei L, Yu SP (2016)
727 Intracranial Transplantation of Hypoxia-Preconditioned iPSC-Derived Neural Progenitor
728 Cells Alleviates Neuropsychiatric Defects After Traumatic Brain Injury in Juvenile Rats.
729 Cell Transplant 25:797-809.
730 Witgen BM, Lifshitz J, Smith ML, Schwarzbach E, Liang SL, Grady MS, Cohen AS (2005)
731 Regional hippocampal alteration associated with cognitive deficit following experimental
732 brain injury: a systems, network and cellular evaluation. Neuroscience 133:1-15.
733 Witkowski ED, Gao Y, Gavsyuk AF, Maor I, DeWalt GJ, Eldred WD, Mizrahi A, Davison IG
734 (2019) Rapid Changes in Synaptic Strength After Mild Traumatic Brain Injury. Front Cell
735 Neurosci 13:166.
736 Wrobel LJ, Reymond-Marron I, Dupre A, Raggenbass M (2010) Oxytocin and vasopressin
737 enhance synaptic transmission in the hypoglossal motor nucleus of young rats by acting on
738 distinct receptor types. Neuroscience 165:723-735.
739 Yager JY, Thornhill JA (1997) The effect of age on susceptibility to hypoxic-ischemic brain
740 damage. Neurosci Biobehav Rev 21:167-174.

741 Yizhar O, Fenno LE, Prigge M, Schneider F, Davidson TJ, O'Shea DJ, Sohal VS, Goshen I,
742 Finkelstein J, Paz JT, Stehfest K, Fudim R, Ramakrishnan C, Huguenard JR, Hegemann P,
743 Deisseroth K (2011) Neocortical excitation/inhibition balance in information processing
744 and social dysfunction. Nature 477:171-178.
745 Zamani A, Ryan NP, Wright DK, Caeyenberghs K, Semple BD (2020) The Impact of Traumatic
746 Injury to the Immature Human Brain: A Scoping Review with Insights from Advanced
747 Structural Neuroimaging. J Neurotrauma 37:724-738.
748 Zhang JB, Chen L, Lv ZM, Niu XY, Shao CC, Zhang C, Pruski M, Huang Y, Qi CC, Song NN,
749 Lang B, Ding YQ (2016) Oxytocin is implicated in social memory deficits induced by
750 early sensory deprivation in mice. Mol Brain 9:98.

751

Figure Legends

Figure 1: Timeline of experiments

Eleven-day-old rat pups were subjected to TBI or sham-injury. Behavioral experiments were conducted in three separate cohorts of animals beginning at either 4 weeks post-injury (adolescent group and oxytocin group) or 8 weeks post-injury (adult group). At the conclusion of the behavioral testing in adolescence, animals were used to generate tissue for qRT-PCR experiments, and animals from the oxytocin group were used for electrophysiological experiments.

Figure 2: Pediatric TBI impaired social recognition but not sociability during adolescence.

Eleven-day-old male and female rat pups were tested for sociability (Stage 2, panels A and C) and social recognition (Stage 3, panels B and D) at 4 weeks after injury (adolescent age) using the three-chamber test as described in the Methods. Data are presented as time (in seconds) spent interacting with rat/object (A and B) or as Discrimination Index (C and D). Open symbols represent sham animals, closed symbols represent injured animals. Bars represent group mean values and the error bars represent standard error of the mean. *, $p<0.05$.

Figure 3: Pediatric TBI impaired social recognition but not sociability during adulthood.

Eleven-day-old male and female rat pups were tested for sociability (Stage 2, panels A and C) and social recognition (Stage 3, panels B and D) at 8 weeks after injury (adult age) using the three-chamber test as described in the Methods. Data are presented as time (in seconds) spent interacting with rat/object (A and B) or as Discrimination Index (C and D). Open symbols represent sham animals, closed symbols represent injured animals. Bars represent group mean values and the error bars represent standard error of the mean. *, $p<0.05$.

774 **Figure 4: Brain-injured animals did not exhibit impairments in novel object recognition**
775 **memory.**

776 At 5 weeks (adolescence, A) and 9 weeks (adulthood, B) following injury, sham- and
777 brain-injured animals were tested for novel object recognition memory as described in the
778 Methods. The Discrimination Index was calculated as described in the Methods. Open symbols
779 represent sham animals, closed symbols represent injured animals. Bars represent group mean
780 values and the error bars represent standard error of the mean.

781 **Figure 5: Expression of mRNAs for oxytocin and oxytocin receptor in adolescence was not**
782 **affected following TBI in 11-day-old rats.**

783 After behavioral testing at 4-5 weeks post-injury, a subset of animals were euthanized and
784 the expression of OXT (A) and OXTR (B) was evaluated in the paraventricular nucleus of the
785 hypothalamus (PVN) and medial prefrontal cortex (PFC) respectively. Open symbols represent
786 sham animals, closed symbols represent injured animals. Expression (ddCT) values were
787 normalized to sham values. Bars represent group mean values and the error bars represent
788 standard error of the mean.

789 **Figure 6: Intranasal administration of oxytocin administration reversed social recognition**
790 **deficits in brain-injured animals in adolescence.**

791 At 30 minutes prior to testing animals in the three-chamber test at 4-5 weeks after injury,
792 sham- and brain-injured animals were administered with saline, oxytocin (oxy) at 20µg, or oxy at
793 60µg as described in the Methods. A) Seconds sniffing in stage 2; B) Seconds sniffing in stage 3;
794 C) Discrimination Index in stage 2; D) Discrimination index in stage 3. E=Empty cup, R=Rat
795 cup, F= Familiar rat, N= Novel rat. Open symbols represent sham rats, filled symbols represent

injured rats, triangles represent vehicle-treated, squares represent 20µg oxy-treated rats, diamonds represent 60µg oxy-treated rats. *, $p<0.05$ in all panels. In panel C, * represents $p<0.05$ compared to brain-injured animals that received saline. Bars represent group mean values and the error bars represent standard error of the mean.

Figure 7: Oxytocin administration did not affect novelty-induced locomotor activity.

At 5 weeks after brain injury and following testing in the three-chamber test, sham- and brain-injured animals were tested for locomotor activity. Animals were administered either saline or oxy 60µg as described in the Methods.

Figure 8: Oxytocin did not affect membrane properties of layer II/III pyramidal neurons within the mPFC.

Following behavioral testing, slices containing the mPFC were obtained at 6-7 weeks after injury and neuronal activity was measured using whole cell patch clamp electrophysiology as described in the Methods. (A) representative current clamp traces from sham and brain-injured neurons; (B) Frequency of neuron firing in response to varying levels of current injection; (C) Rheobase; (D) Input resistance; (E) Membrane voltage; (F) spike threshold. Bars represent mean group values and error bars represent standard error of the mean. Open triangles represent sham cells bathed with aCSF (N=12), open squares represent sham cells bathed with 1 µM OXT (N=6), filled triangles represent injured cells bathed with aCSF (N=13) and filled squares represent injured cells bathed with oxytocin (N=10). *, $p<0.05$.

Figure 9: Oxytocin did not affect spontaneous EPSCs in layer II/III neurons within the mPFC.

(A) Representative traces of spontaneous EPSCs recorded from layer II/III pyramidal neurons within the mPFC. (B) Frequency of spontaneous EPSCs. (C) Amplitude of spontaneous EPSCs. Bars represent group mean value and error bars represent standard error of the mean. Open triangles represent sham cells bathed with aCSF (N=16), open squares represent sham cells bathed with 1 μM OXT (N=11), filled triangles represent injured cells bathed with aCSF (N=20), filled squares represent injured cells bathed with 1 μM OXT (N=19).

Figure 10: Oxytocin increased the frequency of spontaneous IPSCs in layer II/III neurons within the mPFC.

(A) Representative traces of spontaneous IPSCs recorded from layer II/III pyramidal neurons within the mPFC. (B) Frequency of spontaneous IPSCs. (C) Amplitude of spontaneous IPSCs. Bars represent group mean value and error bars represent standard error of the mean. Cumulative probability of small IPSC frequencies in sham (D) and injured cells (E). (F-G) Cumulative probability of large IPSC frequencies in sham (F) and injured cells (G). Cumulative probability of small IPSC amplitudes in sham (H) and injured cells (I). Cumulative probability of large IPSC amplitudes in sham (J) and injured cells (K) (Ryan et al., 2016; Douglas, 2020) (Ryan et al., 2016; Douglas, 2020) (Ryan et al., 2016; Douglas, 2020) (Ryan et al., 2016; Douglas, 2020) (Ryan et al., 2016; Douglas, 2020). Open triangles represent sham cells bathed with aCSF (N=13), open squares represent sham cells bathed with 1 μM OXT (N=12), filled triangles represent injured cells bathed with aCSF (N=17), filled squares represent injured cells bathed with 1 μM OXT (N=15). * = $p<0.05$.

FIGURE 1

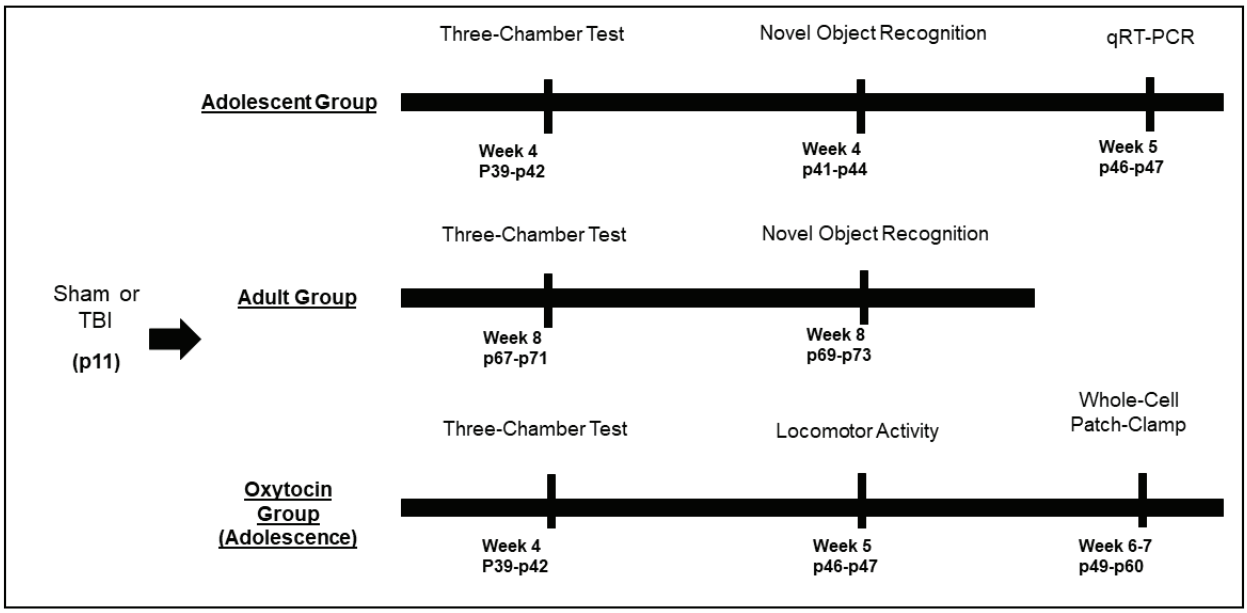

FIGURE 2

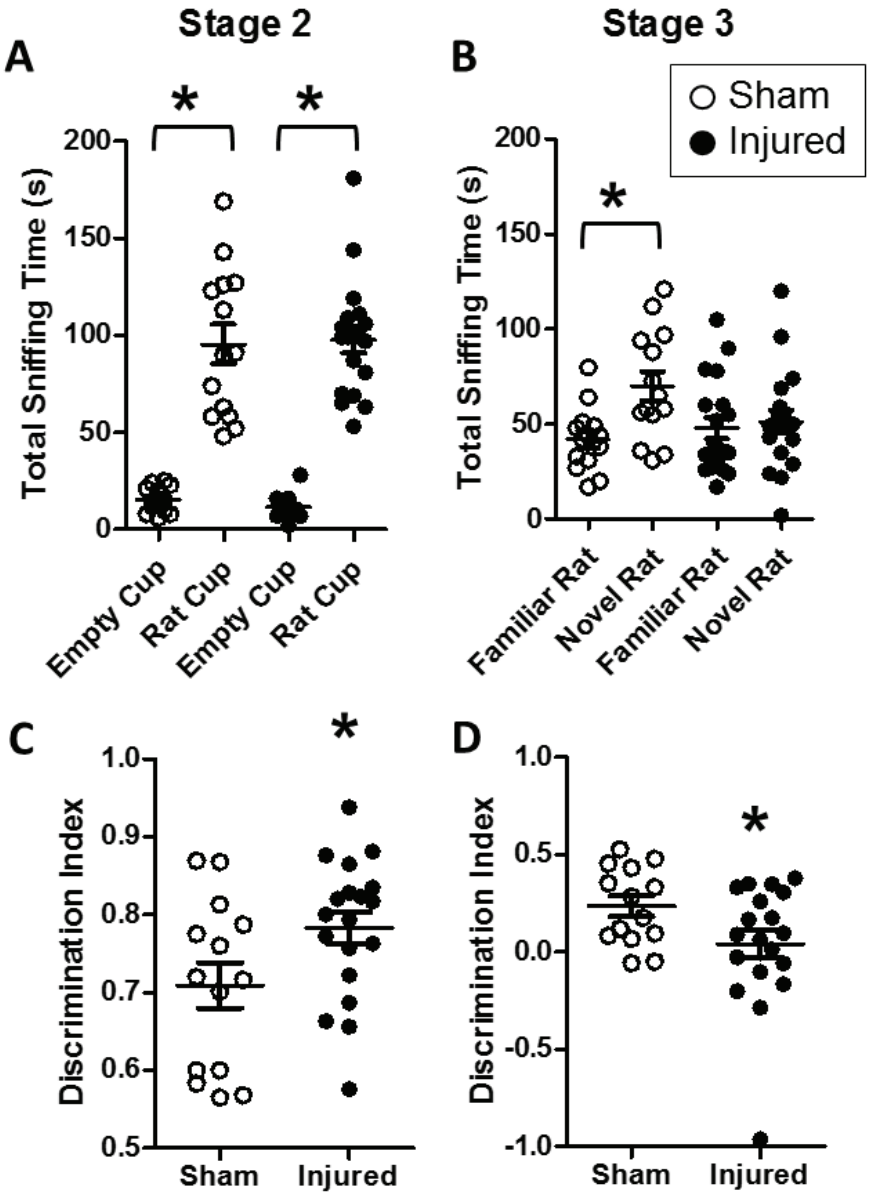

FIGURE 3

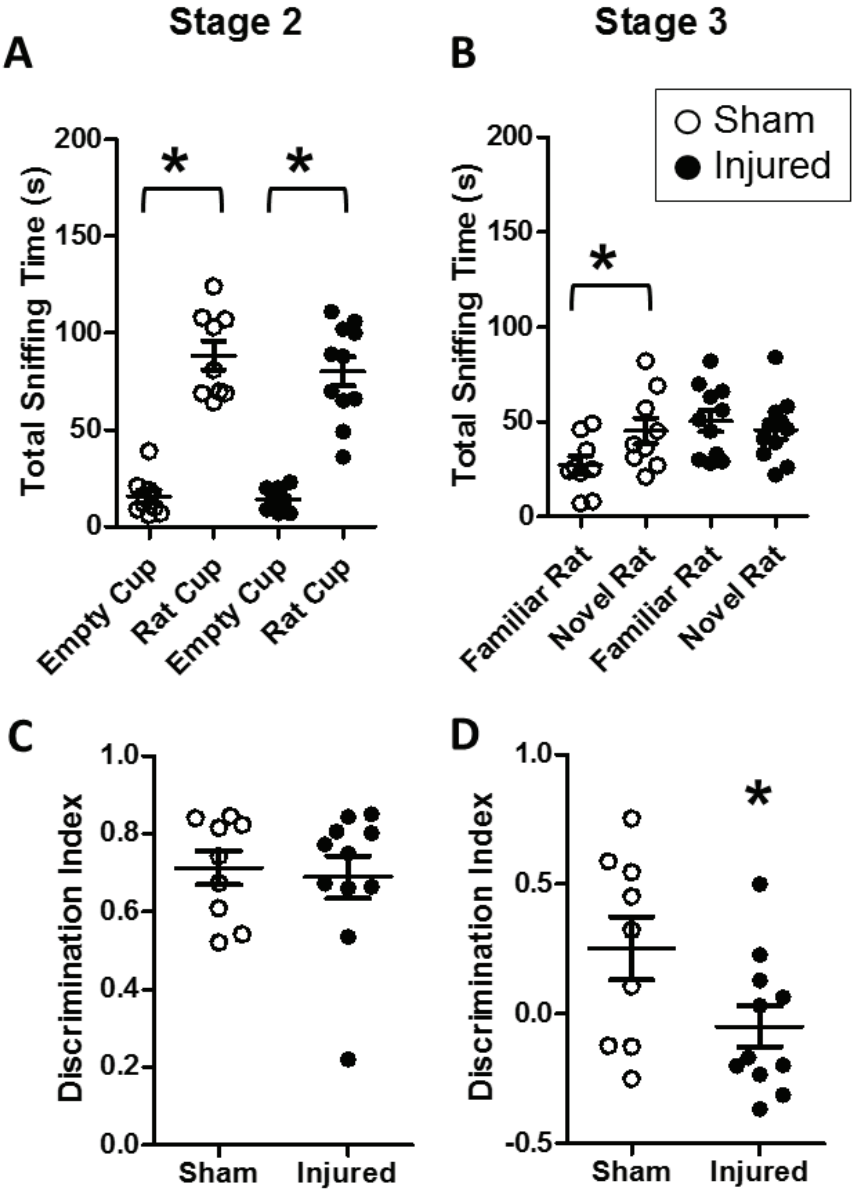

FIGURE 4

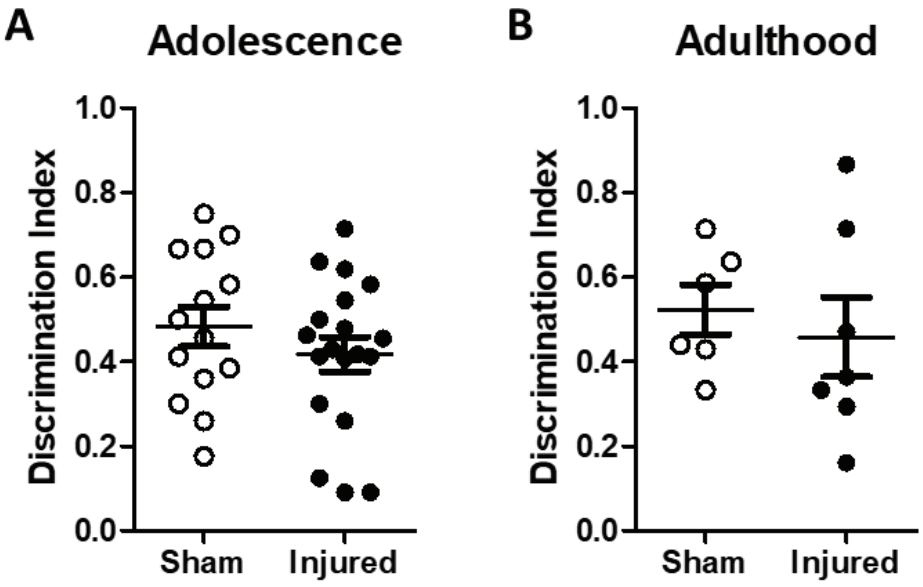

FIGURE 5

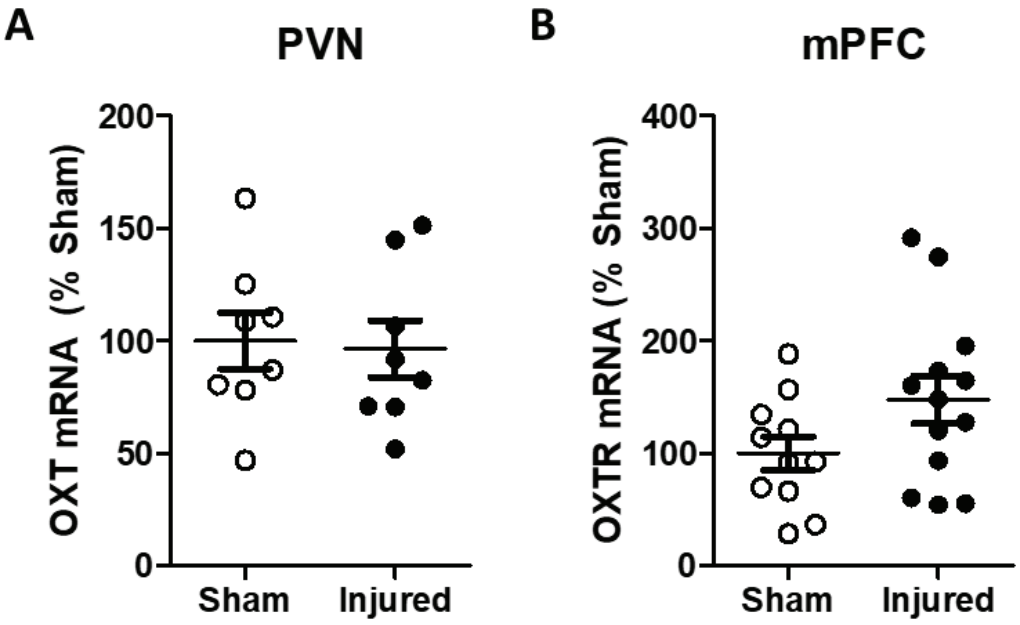

FIGURE 6

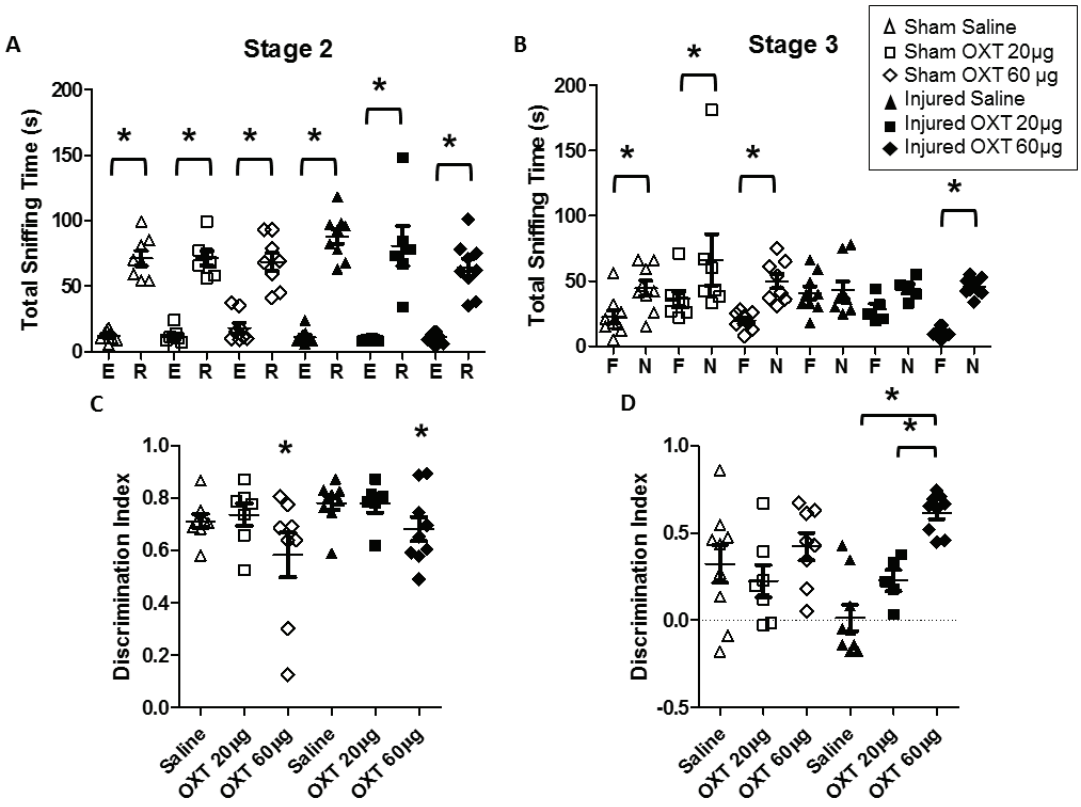

FIGURE 7

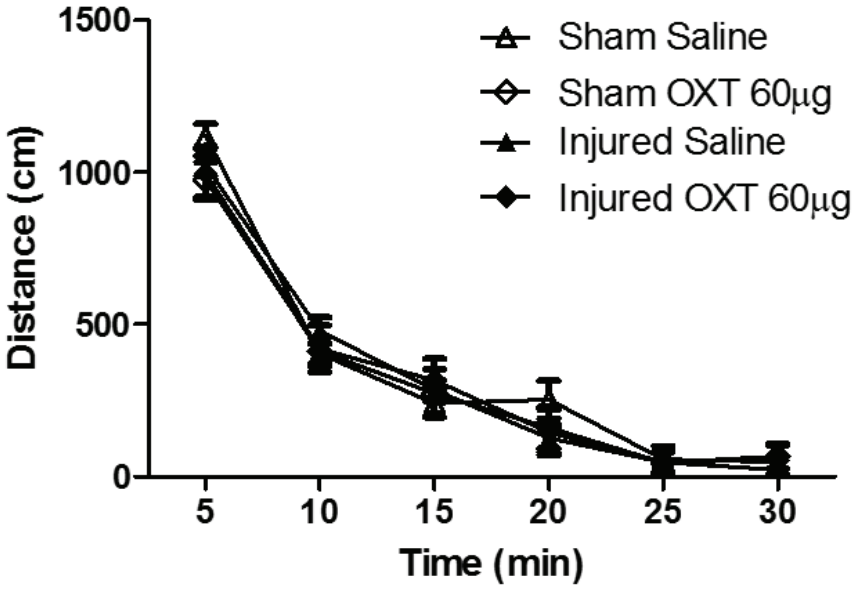

FIGURE 8

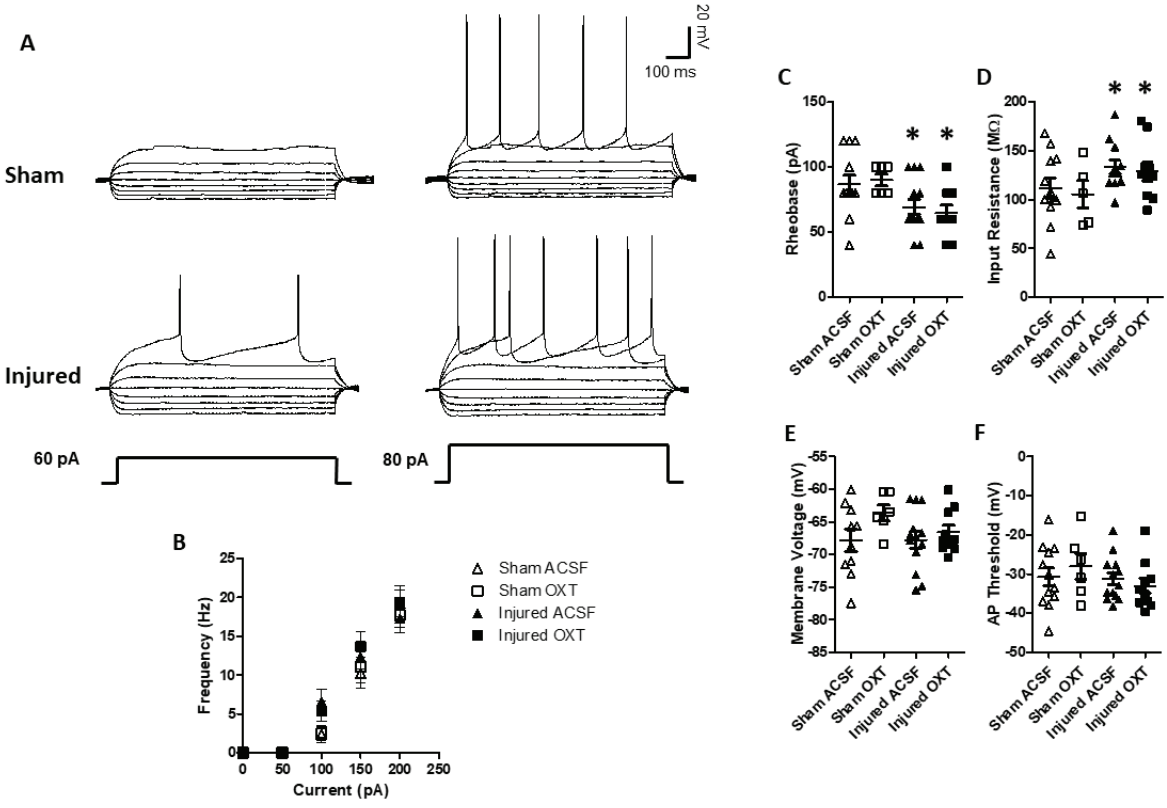

FIGURE 9

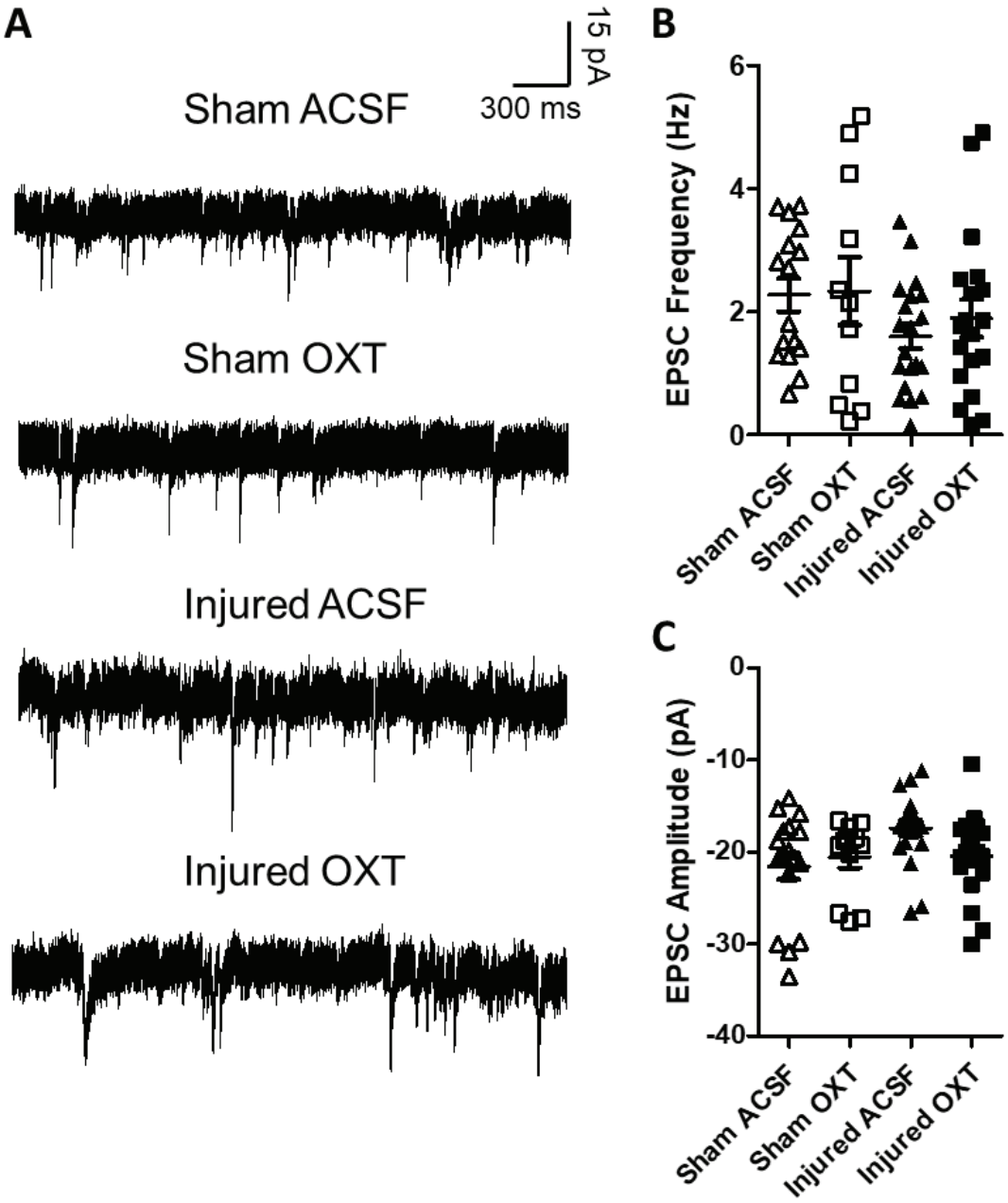

FIGURE 10

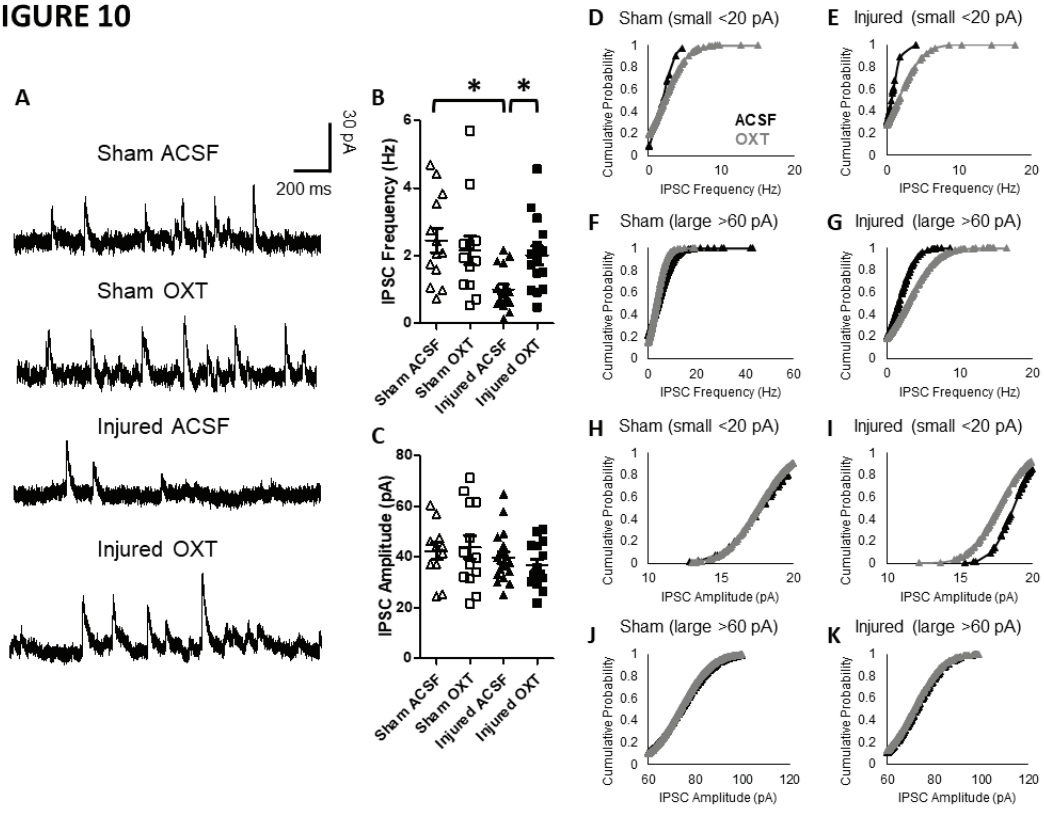

Table 1: Acute neurologic status of rats in the study.

Eleven-day-old male and female rat pups were randomly assigned to either sham- or brain-injured groups. Sham- and brain-injured rats were randomly assigned to receive intranasal administration of 20 µg (1x) or 60 µg (3x) oxytocin. Subsets of the animals tested in the behavioral assays were randomly assigned to be euthanized for mRNA measurements and whole-cell patch clamp electrophysiology. Latency to regain righting reflex and times of apnea were recorded as described in the Methods. *, $p<0.05$ compared to sham-injured rats.

*males+females

Outcome	Group	N	Righting reflex (s)	Apnea (s)
Behavior (Adolescence)	Sham	16	69 ± 9	NA
	Injured	20	284 ± 40*	10 ± 2
Behavior (Adult)	Sham	12	70 ± 11	NA
	Injured	12	151 ± 16*	13 ±1
Behavior (Oxytocin)	Sham + Saline	9	97 ± 24	NA
	Sham + OXT 1x	7	119 ± 22	NA
	Sham + OXT 3x	8	79 ± 15	NA
	Injured + Saline	10	301 ± 32*	5 ± 1
	Injured+OXT 1x	7	306 ± 99*	6 ± 3
	Injured+OXT 3x	10	320 ± 50*	16 ± 4*